NORSAR

NORSAR Scientific Report No. 2-2011

Semiannual Technical Summary

1 January - 30 June 2011

Frode Ringdal (ed.)

Kjeller, August 2011

6.2 The Novaya Zemlya event on 11 October 2010

6.2.1 Introduction

The area around the archipelago of Novaya Zemlya is considered to be relatively aseismic. However, since Novaya Zemlya was the site of many years of extensive nuclear testing by the former Soviet Union, there has been a considerable interest in analysis and classification of all seismic events occurring in this region. Apart from the large explosions at the known test sites, there have during the last decades only been two events with magnitudes larger than 4. An analysis of the m_b 4.7 event on 1 August 1986, located on the east coast of the island (see Figure 6.2.1), was published by Marshall et. al, 1989.

On 11 October 2010, at 22:48:25.6 (IDC_REB), an event with magnitude 4.3 (IDC_REB) occurred on the north-west coast of Novaya Zemlya. The event was well recorded globally, and phase readings at 44 IMS stations contributed to the REB location. It has previously been observed that there is very efficient propagation of high-frequency signals for ray-paths crossing the Barents Sea (Ringdal et. al, 2008). As a consequence, both the IMS seismic stations on Svalbard (the SPITS array) and in northern Norway (the ARCES array) have been equipped with instruments having sampling rates of 80 Hz and 100Hz, respectively. In addition to an assessment of the reported event locations, we will in this contribution present the high-frequency recordings at SPITS and ARCES.

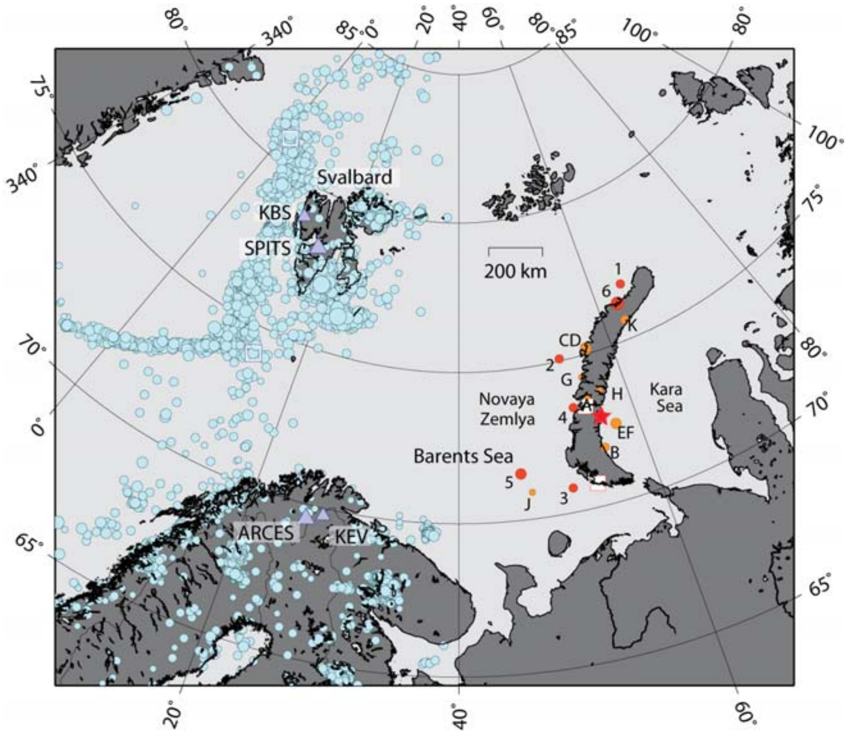

Fig. 6.2.1. Map showing the location of the SPITS and ARCES array, seismic events near Novaya Zemlya since 1992 (red/orange filled circles), and the seismicity of the region as reported in NORSAR's monthly seismic bulletin 1998-2008 (blue filled circles). The 1 August 1986 event is marked by a red star, and the 11 October 2011 event is labelled by the number 6. The figure is adapted from Gibbons et. al, 2011.

6.2.2 Location estimates

The IDC reviewed event bulletin (REB) reports the following hypcenter information for the 11 October 2010 event:

Origin time (UTC)	2010/10/11 22:48:25.62
Location	76.2640N; 64.7619E
Location errors (km)	Smaj10.6; Smin 8.6; Az 160
Depth	0 (Fixed)
Magnitude	$mb1_{mx}$ 4.3; $ms1_{mx}$ 3.2

The REB location and the associated error ellipse is shown red in Figure 6.2.2. The NEIC location is shown by a green symbol. The REB location is mainly based on readings at distant stations. ARCES is the only station within 2000 km of the event that contributed to the REB location, and surprisingly the high-quality recordings at the SPITS array were not used in the REB.

Phase picks at regional distance stations, on Svalbard and in northern Fennoscandia, dominated the input to the initial location reported in NORSAR's regional bulletin. This location, differed significantly, by about 65 km, from the REB location (see black symbol in Figure 6.2.2). In an attempt to combine phase readings at both regional and teleseismic distances, we relocated the event using the re-picked phases listed in Table 6.2.1. The location was calculated with the HYPOSAT program of Schweitzer, 2001, using a combination of the regional *"barey"* model (Schweitzer and Kennett, 2007) and the global *"AK135"* model. The recalculated location differed by 22 km from the REB location (see blue symbol in Figure 6.2.2). The following hypocentral parameters were obtained:

Origin time (UTC)	2010/10/11 22:48:27.725
Location	76.2999N; 63.9627E
Location errors (km)	Smaj6.3; Smin 5.6; Az 39
Depth	0 (Fixed)

The distances to the stations used for the event relocation were all exceeding 900 km from the event epicenter. The stations at regional distances (within 2000 km) cover a very narrow azimuth range (240-310 degrees) in the westerly direction from the event (see Table 6.2.1). As a result, a small error in the propagation velocities of the one-dimensional location model may cause in a significantly biased location. This is particularly apparent for NORSAR's initial event location, shown by the black symbol of Figure 6.2.1. We conclude that there is a need to improve the regional location models used for routine data analysis of events, and use of existing three-dimensional regional propagation models in this analysis should be encouraged.

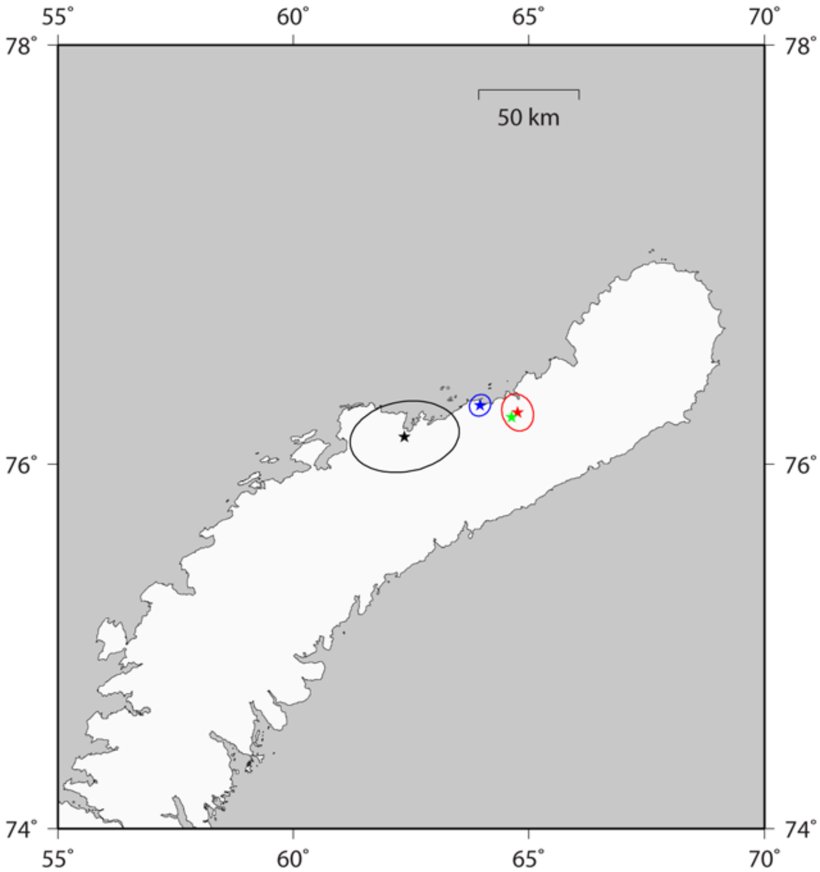

Fig. 6.2.2. Location estimates of the 11 October 2010 event.
Red: IDC Reviewed Event Bulletin
Green: NEIC
Black: NORSAR's regional reviewed bulletin
Blue: NORSAR's relocation using a combination of regional and teleseismic data

Table 6.2.1. Phase readings used for relocating the 10 October 2010 event

Stat	Delta	Azi	Phase	[used]	Onset time	Res	Baz	Res	Rayp	Res	Used
HOPEN	9.050	290.22	Sn		22 52 13.088	-2.433					T
SPITS	10.437	302.81	Pn		22 50 56.091	1.051	70.89	-5.39	14.46	1.12	T D
SPITS	10.437	302.81	Sn		22 52 47.634	-0.704	90.70	14.42	24.82	1.19	T D
HSPB	10.957	297.00	P1	Pn	22 51 1.474	-0.435					T D
HSPB	10.957	297.00	S1	Sn	22 52 57.697	-2.808					T D
TER	10.984	244.78	Pn		22 51 2.815	0.524	13.11	-24.03	9.14	-4.19	T D
TER	10.984	244.78	Sn		22 52 57.835	-3.348					T D
KBS	11.123	307.82	Pn		22 51 5.333	1.198	99.58	22.72	2.90	-10.43	T D
KBS	11.123	307.82	Sn		22 53 4.249	-0.197					T D
LVZ	12.149	241.68	Pn		22 51 18.810	0.918					T
LVZ	12.149	241.68	Sn		22 53 25.349	-3.447					T
KEV	12.381	257.42	P1	Pn	22 51 21.451	0.568	45.64	3.70	12.81	-0.50	TASD
KEV	12.381	257.42	S1	Sn	22 53 31.542	-2.555					T D
ARA0	12.896	258.54	P1	Pn	22 51 28.074	0.298	54.09	12.47	11.51	-1.80	T D
ARA0	12.896	258.54	S1	Sn	22 53 43.107	-3.184	50.72	9.10	17.71	-5.84	T D
VRF	13.363	248.42	Pn		22 51 34.783	0.813	30.83	-4.76	10.55	-2.75	TA D
VRF	13.363	248.42	Sn		22 53 55.670	-1.582					T D
HEF	14.191	257.57	Pn		22 51 45.080	0.114	34.53	-4.43	8.63	-4.66	TA D
HEF	14.191	257.57	Sn		22 54 14.382	-2.321					T D
KIF	14.372	262.48	Pn		22 51 48.278	0.897	43.18	2.12	11.03	-2.26	TA D
KIF	14.372	262.48	Sn		22 54 19.118	-1.856					T D
TRO	14.380	266.10	Pn		22 51 49.359	1.953	16.85	-25.94	11.01	-2.28	T
TRO	14.380	266.10	Sn		22 54 16.682	-4.341					T
KU6	14.743	244.10	Pn		22 51 53.484	1.203	42.93	11.28	12.92	-0.36	T SD
KU6	14.743	244.10	Sn		22 54 28.673	-0.972					T D
LANU	14.862	258.62	Pn		22 51 54.065	0.184	10.89	-27.53	5.83	-7.45	T D
LANU	14.862	258.62	Sn		22 54 32.148	-0.325					T D
MSF	15.024	245.02	Pn		22 51 57.138	1.123	35.06	3.30	11.60	-1.68	TA
DAG	17.822	311.71	P1	Pn	22 52 33.727	0.801	53.72	3.14	13.68	0.46	TAS
DAG	17.822	311.71	S1	Sn	22 55 32.510	-9.044					
FINES	19.592	241.64	P1	P	22 52 55.090	0.661	22.18	-3.70	12.80	1.85	TA
ARU	20.057	188.77	P		22 53 0.194	0.639	353.07	-10.68	13.27	2.35	T
CHKZ	22.860	169.78	P		22 53 29.348	-0.379	359.49	3.57	10.64	0.02	TASD
CHKZ	22.860	169.78	S		22 57 33.147	-1.212					T D
NC400	23.123	258.13	P		22 53 34.966	2.437	17.95	-10.73	6.34	-4.24	T
NB200	23.276	258.63	P		22 53 36.194	2.024	29.98	1.29	9.53	-1.03	TA
NBO00	23.386	259.09	P		22 53 37.160	1.860	30.06	1.33	8.38	-2.17	TA
NC600	23.477	258.01	P		22 53 37.806	1.583	20.52	-7.82	8.67	-1.87	T
BVAR	23.502	170.24	P		22 53 35.720	-0.838	5.31	9.15	7.75	-2.78	T
ZRNK	23.526	172.34	P		22 53 36.321	-0.483					T D
ZRNK	23.526	172.34	S		22 57 48.312	1.615					T D
NAO00	23.555	258.78	P		22 53 38.402	1.343	24.34	-4.16	9.24	-1.28	TA
ZALV	23.793	148.56	P		22 53 37.908	-1.604	341.33	-6.53	8.78	-0.37	T S
VOS	23.828	169.40	P1	P	22 53 38.917	-0.933	10.94	15.07	12.36	3.21	T
AKTO	26.073	188.67	P1	P	22 54 0.276	-0.012					T
KURK	26.329	158.73	P1	P	22 54 2.644	0.060	356.42	4.24	8.31	-0.74	TAS
ABKAR	27.194	185.77	P		22 54 10.768	0.376	343.61	-18.49	9.39	0.39	T S
AKASG	29.076	228.25	P1	P	22 54 27.109	-0.053	18.63	2.40	9.55	0.67	TAS
MKAR	30.559	154.85	P		22 54 39.405	-0.994	352.76	1.24	7.69	-1.15	TA
EKA	31.817	267.81	P1	P	22 54 52.885	1.545	25.57	0.95	8.93	0.13	TAS
BURAR	32.763	231.49	P1	P	22 55 1.064	1.201	4.61	-11.39	7.64	-1.12	T
SONM	33.260	124.02	P1	P	22 55 3.580	-0.674	334.54	-8.41	8.69	-0.05	T S
KKAR	33.418	171.28	P1	P	22 55 6.158	0.637					T
USP	33.443	165.97	P1	P	22 55 6.349	0.578	343.10	-12.36	5.72	-3.01	T
CHM	33.725	165.68	P1	P	22 55 9.289	1.074	358.40	3.01	7.31	-1.40	TA
GERES	33.934	245.52	P1	P	22 55 12.175	2.132	29.72	10.55	9.02	0.32	T S
EKS2	34.006	167.01	P1	P	22 55 11.043	0.257					T
AAK	34.076	166.09	P1	P	22 55 12.572	1.413					T
UCH	34.479	166.10	P1	P	22 55 16.872	1.539	356.77	1.19	5.60	-3.07	TA
AML	34.530	167.18	P1	P	22 55 17.553	1.857	347.40	-8.52	7.62	-1.04	T
KZA	34.672	165.16	P1	P	22 55 17.858	0.915					T
INK	35.210	11.17	P1	P	22 55 20.239	-0.481	9.33	16.46	3.90	-4.72	T
ILAR	37.836	20.99	P1	P	22 55 43.333	0.117	345.53	-2.98	7.63	-0.83	TAS
GEYT	38.558	187.42	P		22 55 50.759	1.144	320.90	-41.33	7.68	-0.73	T S
ESDC	46.630	259.67	P1	P	22 56 56.876	1.641	15.34	-2.35	9.65	1.80	TA
KEST	47.395	244.32	P1	P	22 57 2.994	1.714					T
MJAR	51.107	95.24	P		22 57 27.214	-2.374	333.98	-8.88	9.75	2.23	T
CMAR	60.633	141.33	P1	P	22 58 36.289	-1.760	341.05	-9.93	7.42	0.59	T S
TORD	70.880	245.86	P1	P	22 59 44.285	0.088	355.81	-17.09	6.88	0.80	T S
TXAR	74.332	348.80	P		23 00 4.992	0.210	7.53	4.49	3.98	-1.85	TA

6.2.3 Spectral characteristics of SPITS and ARCES observations

The SPITS and the ARCES arrays are located at distances of 1178 and 1451 km, respectively, from the event epicenter (REB location). Waveforms, phase spectra and spectrograms for the SPITS and ARCES observations are shown in Figures 6.2.3 - 6.2.7. For the SPITS recordings, the presence of significant energy up to the Nyquist frequency of 40 Hz confirms the documented efficient high-frequency wave propagation from the Novaya Zemlya region to Svalbard, across the Barents Sea (Ringdal et. al, 2008).

For the ARCES high-frequency element, installed in March 2008, there has so far only been recorded two events from the eastern Barents Sea/Novaya Zemlya region. The magnitude 3.2 event on 11 November 2009 located in the eastern Barents Sea (labelled 5 in Figure 6.2.1), showed significant energy event up to 40 Hz both for the Pn and Sn phases (Kværna and Ringdal, 2010). The epicentral distance from ARCES to the 11 November 2009 event was about 800 km.

The 10 October 2010 event was located at a distance of about 1450 km from the ARCES array, and the spectra show signal energy up to about 25 Hz for the Pn and Sn phases. As compared to the SPITS spectra and the ARCES spectra of the 11 November 2009 event, the ARCES spectra for this event has comparatively less high frequency energy. We attribute this to a longer propagation path, and to signal attenuation when the seismic waves crossed the heterogeneous crustal structures of the Novaya Zemlya island. However, we nevertheless consider this as very efficient propagation of high-frequency energy.

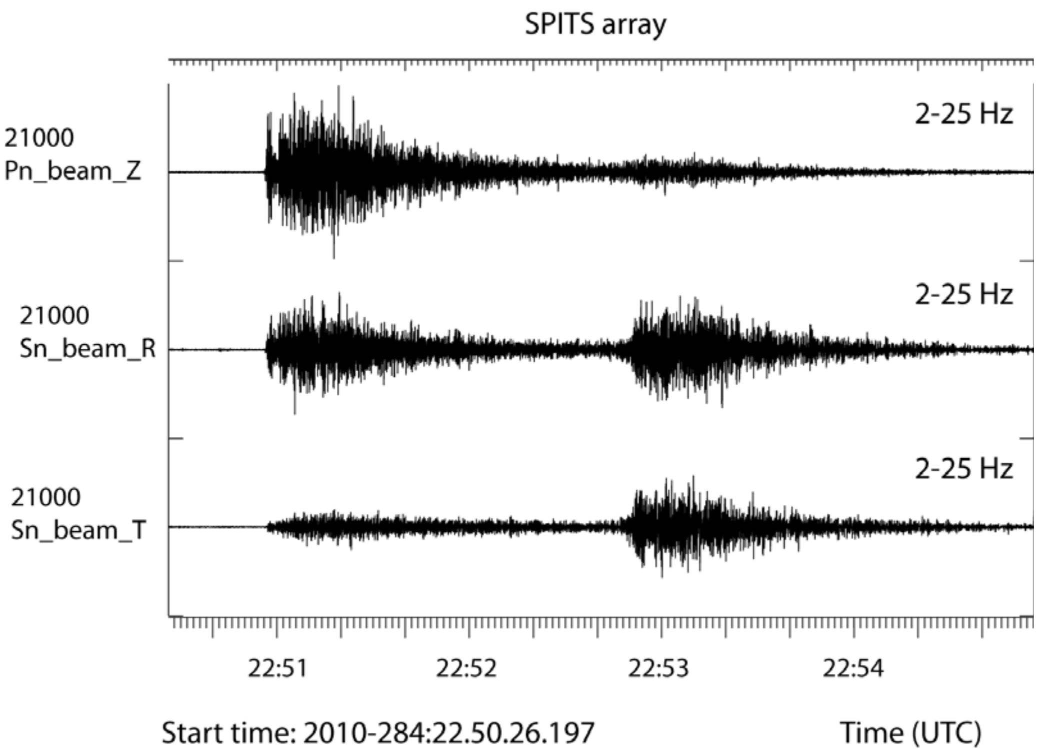

Fig. 6.2.3. Waveforms from the 11 October 2011 event recorded at the SPITS array. The upper trace shows the Pn beam of the 9 vertical-component sensors. The middle trace shows the Sn-beams of the 6 horizontal component sensors after rotation into the radial direction of the incoming wave. The lower trace shows the corresponding Sn beam of the transversely rotated horizontal sensors.All traces are bandpass filtered between 2 and 25 Hz.

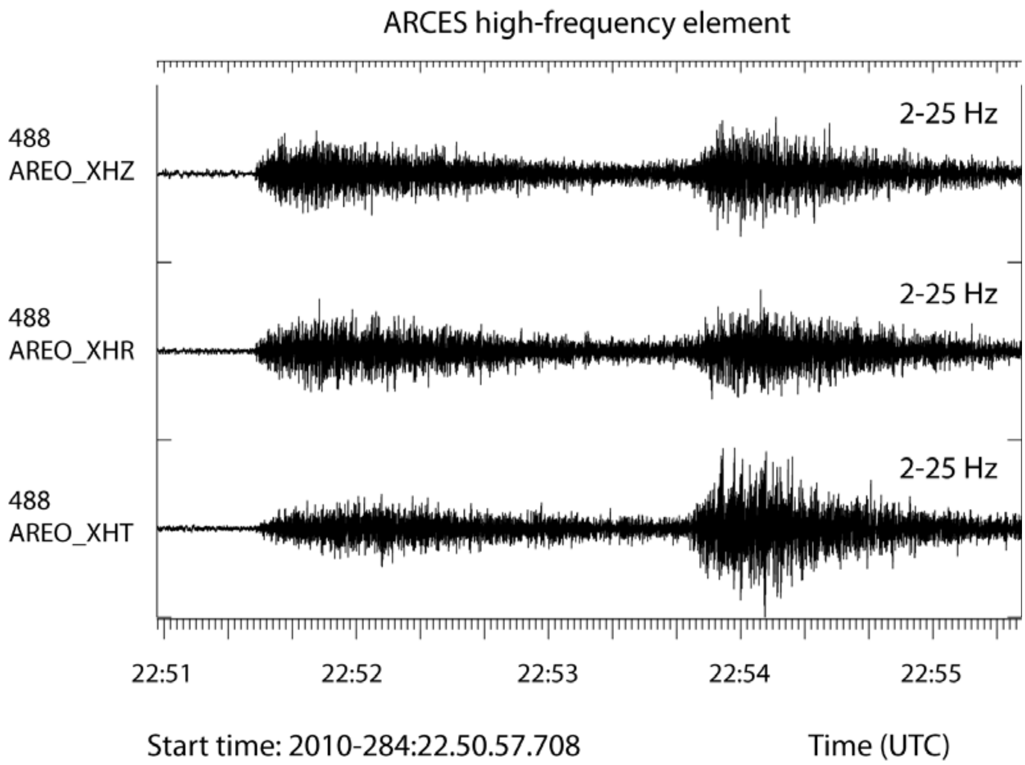

Fig. 6.2.4. Waveforms from the 11 October 2011 event recorded at the ARCES high-frequency element ARE0. The upper trace shows the vertical component sensor. The two lower traces show the horizontal components after rotation into the radial and transverse directions. All traces are bandpass filtered between 2 and 25 Hz.

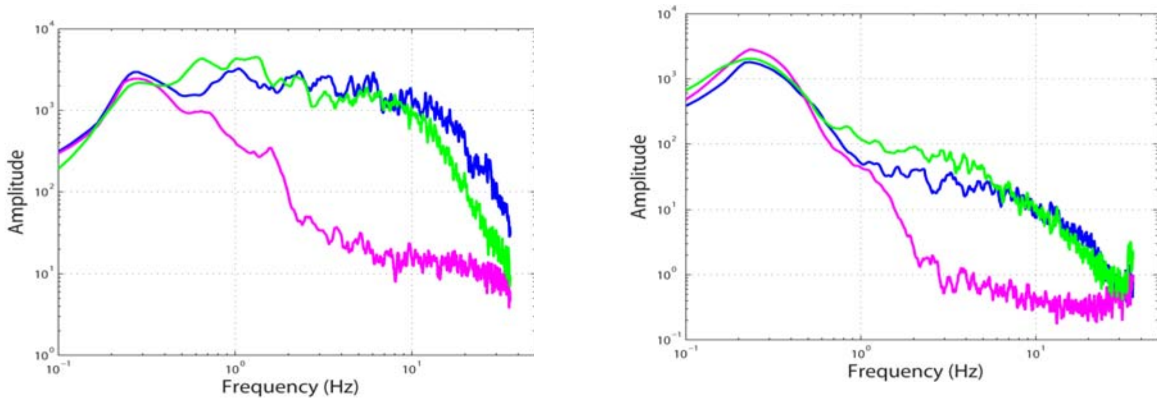

Fig. 6.2.5. Left: Spectra from the SPA0 three-component sensor of the SPITS array of the Pn (blue) and Sn (green) phases of the 11 October 2010 event. The noise spectrum (magenta) preceding the event is also shown. The Pn and noise spectra are calculated from the vertical component sensor, whereas the Sn spectrum is calculated from the transverse horizontal component.
Right: Corresponding spectra for the ARE0 high-frequency three-component sensor of the ARCES array. Time windows of 60 seconds were used for calculating all spectra.

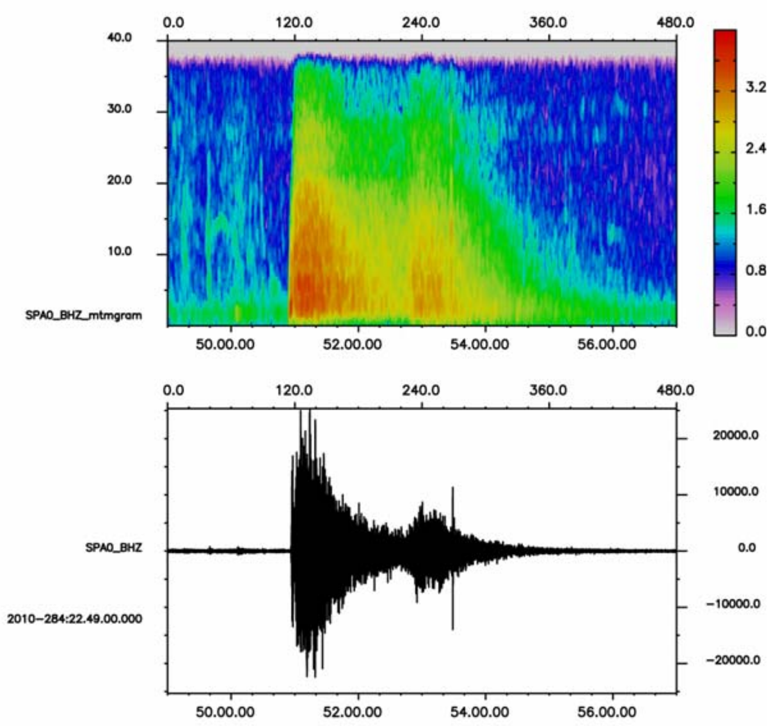

Fig. 6.2.6. Spectrogram for the vertical-component sensor SPA0_BHZ of the SPITS array for an eight minutes time interval around the P and S phases of the 11 October 2010 event.

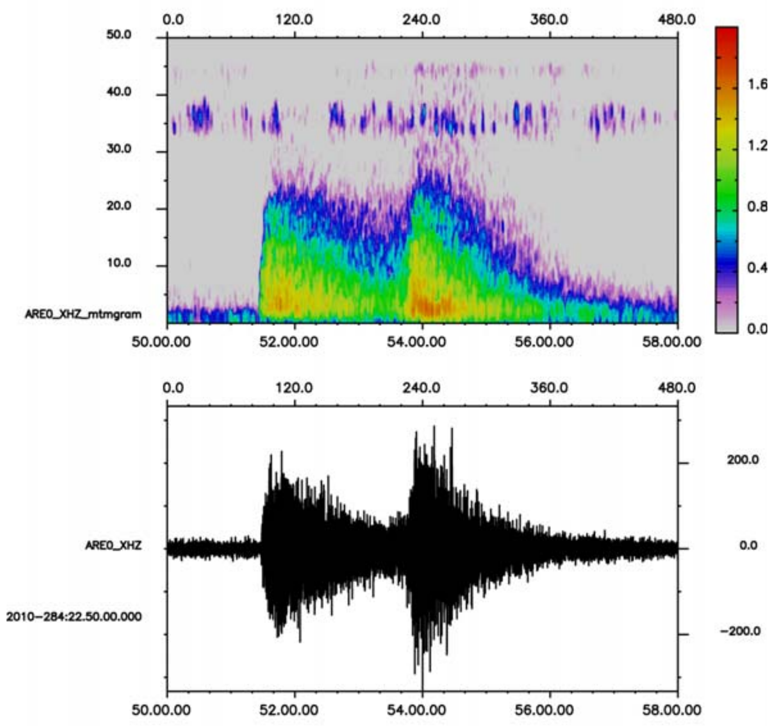

Fig. 6.2.7. Spectrogram for the vertical-component sensor ARE0_XHZ of the ARCES array for an eight minutes time interval around the P and S phases of the 11 October 2010 event.

References

Gibbons, S.J., J. Schweitzer, F. Ringdal, T. Kværna, S. Mykkeltveit and B. Paulsen (2011). Improvements to Seismic Monitoring of the European Arctic Using Three-Component Array Processing at SPITS. To be published in BSSA, December 2011.

Kværna, T. and F. Ringdal (2010). Seismic event in the Barents Sea, 11 November 2009. *In NORSAR Scientific Report No. 1-2010: Semiannual Technical Summary, NORSAR, Kjeller, Norway.*

Ringdal, F., Kværna, T., and Gibbons, S. J. (2008). Initial studies of high-frequency signals recorded at ARCES infrasound sensors. *In NORSAR Scientific Report No. 2-2008: Semiannual Technical Summary, NORSAR, Kjeller, Norway.*

Schweitzer, J. (2001): HYPOSAT – An Enhanced Routine to Locate Seismic Events. *Pure and Applied Geophysics,* **158**, No. 1, 277-289.

Schweitzer, J. and B.L.N. Kennett (2007). Comparison of Location Procedures: The Kara Sea Event of 16 August 1997. *Bull. Seism. Soc. Am.*, **97**, No. 2, 389-400.

Tormod Kværna
Steven Gibbons